2026, Scienceline Publication
World's Veterinary Journal
World Vet J, 16(1): 191-200.
ISSN 2322-4568

DOI: https://dx.doi.org/10.54203/scil.2026.wvj18
PII: S232245682600018-16

Effects of Fermented *Crescentia cujete* on Urinalysis, *Cyclooxygenase-2*, *Vascular Endothelial Growth Factor*, and Renal Function in Unilateral Hydronephrotic Rats

Oscar Maulana Pribadi[1,2], Yos Adi Prakoso[2*], Agustina Dwi Wijayanti[3], Achmadi Susilo[4], and Sitarina Widyarini[5]

[1]*Master Program in Veterinary Sciences, Faculty of Veterinary Medicine, University of Gadjah Mada, Yogyakarta, 55281, Indonesia*
[2]*Department of Pharmacology, Faculty of Veterinary Medicine, University of Wijaya Kusuma Surabaya, 60225, Indonesia*
[3]*Department of Pharmacology, Faculty of Veterinary Medicine, University of Gadjah Mada, 55281, Indonesia*
[4]*Department of Agrotechnology, Faculty of Agriculture, University of Wijaya Kusuma Surabaya, 60225, Indonesia*
[5]*Department of Pathology, Faculty of Veterinary Medicine, University of Gadjah Mada, 55281, Indonesia*

*Corresponding author's E-mail: yos.vet.docter@gmail.com

ORIGINAL ARTICLE
Received: December 28, 2025
Revised: February 04, 2026
Accepted: February 28, 2026
Published: March 31, 2026

ABSTRACT

Unilateral ureteral obstruction (UUO) leads to increased intraluminal pressure, causing a compensatory impact on the contralateral kidney. Common treatments involving diuretics and surgical interventions often fail to offer a complete resolution of the underlying renal damage. Fermented *Crescentia cujete* (FCC), an herbal-derived product with multifaceted therapeutic benefits, presents a potential alternative treatment. The present study aimed to evaluate the potential of FCC to protect renal function using UUO rat models. The study employed 30 male *Sprague Dawley* rats (6 months old, weighing 253.76 ± 8.32 g) which were distributed randomly into five distinct groups, including a healthy control (T1), a sham-operated group (T2), an untreated UUO group (T3), a group receiving UUO plus 92.5 mg/kg BW Prive Uricran® (T4), and a group receiving UUO plus 5.92 mg/kg BW FCC (T5). The test subjects received oral gavage treatment twice daily over a period of 14 days. On day 15, serum and urine were assessed to assess blood urea nitrogen (BUN) and creatinine concentrations, and urinalysis. Moreover, the rats were euthanized, and the kidney tissue was harvested to assess the immunoexpression of *cyclooxygenase-2* (*COX-2*) and *vascular endothelial growth factor* (*VEGF*). The results showed that unilateral hydronephrosis caused significant renal impairment in the untreated group (T3) compared to the healthy (T1) and sham (T2) groups. The changes in the T3 group were characterized by marked elevations in BUN and creatinine, deteriorated urinalysis profiles, and a surge in *COX-2* and *VEGF* immunoexpression. Therapeutic intervention with FCC (T5) successfully mitigated compensatory effects, demonstrating a capacity to restore urinalysis parameters to levels compared to T1 and T2. Furthermore, the treatment effectively downregulated *COX-2* and *VEGF* immunoexpression in the contralateral renal tissue, reducing them to levels statistically indistinguishable from those of the healthy control. The present findings confirmed that FCC has a reno-protective activity on the contralateral kidney following UUO induction, evidenced by stabilized urinalysis profiles and suppressed *COX-2* and *VEGF* immunoexpression.

Keywords: *Cyclooxygenase*-2, Fermented *Crescentia cujete*, Hydronephrosis, Unilateral ureteral obstruction, *Vascular endothelial growth factor*

INTRODUCTION

The kidneys play a critical role in maintaining physiological homeostasis by regulating extracellular electrolyte concentrations and managing excretion through the glomerular filtration rate (GFR, Scott and Quaggin, 2015). However, these essential functions can be severely disrupted by ureteral obstruction (Mohammadi-Sichani et al., 2022). Ureteral obstruction (UO) is a condition that precipitates hydronephrosis, which is the swelling of the kidney due to fluid accumulation (Tannuri et al., 2025). Ureteral obstruction can occur either bilaterally (BUO) or unilaterally (UUO). The obstruction in UUO leads to increased luminal pressure and triggers irreversible tubular dysfunction (Nakamura et al., 2024). Unmitigated chronic obstruction exacerbates fibrosis and inflammation, potentially culminating in renal failure as the compensatory capacity of the contralateral kidney is overwhelmed (Kumar et al., 2015). Contemporary therapeutic strategies, encompassing both surgical procedures and pharmacological agents such as diuretics, predominantly focus on preserving renal function rather than providing a definitive curative solution for the intrinsic pathological damage (Haberal and Tonyali, 2024; Siregar et al., 2024).

From a molecular perspective, the maintenance of renal homeostasis is critically modulated by *cyclooxygenase-2* (*COX-2*, Zhang et al., 2018) and *vascular endothelial growth factor* (*VEGF*, Chade, 2017). *Cyclooxygenase-2* is essential for modulating renal hemodynamics (Kirkby et al., 2018), while *VEGF* acts as a key regulator of glomerular microvascular integrity (Advani et al., 2007). Demonstrated that *COX-2* overexpression during UUO in rat models promotes fibrogenesis and exacerbates renal fibrosis (Tofteng et al., 2022). Moreover, a previous study by Zeisberg et al.

To cite this paper: Pribadi OM, Prakoso YA, Wijayanti AD, Susilo A, and Widyarini S (2026). Effects of Fermented *Crescentia cujete* on Urinalysis, *Cyclooxygenase-2*, *Vascular Endothelial Growth Factor*, and Renal Function in Unilateral Hydronephrotic Rats. *World Vet. J.*, 16(1): 191-200. DOI: https://dx.doi.org/10.54203/scil.2026.wvj18

(2008) indicated that *VEGF* promotes fibrosis within the renal interstitium in hydronephrosis via its capacity to transition renal tubular epithelia-mesenchymal. An excessive synergy between the two factors can lead to over-filtration, which may induce hypotension and further burden GFR mechanisms. Consequently, controlling the immunoexpression of *COX-2* and *VEGF* is crucial for stabilizing renal function during obstruction (Doi et al., 2010; Tofteng et al., 2022).

A promising approach to mitigate the molecular over expression involves the use of antioxidants derived from the fermentation of the Calabash tree fruit (*Crescentia cujete* L.; Oladunjoye et al., 2025). Fermented *Crescentia cujete* (FCC) contains essential bioactive compounds, including retinol, choline, phytonadione, and α-tocopherol, which have been shown to suppress systemic inflammation through modulation of the *cyclooxygenase* pathway (Prakoso et al., 2024; Prakoso et al., 2025). Specifically, choline has been linked to the initiation of GFR recovery (Baris et al., 2023). While, α-tocopherol and retinol exert protective effects and contribute to the repair of renal injury by inhibiting nephropathy processes (Baltusnikiene et al., 2023; DiKun and Gudas, 2023). Despite these established effects, the precise mechanisms through which components of FCC modulate the *COX-2* and *VEGF* signaling pathways in hydronephrosis remain unclear largely unclear. Therefore, the present study aimed to analyze the efficacy of FCC on kidney function and the immunoexpression of *COX-2* and *VEGF* in a rat model of UUO.

MATERIALS AND METHODS

Ethical approval

All experimental protocols involving animal subjects in the current study received ethical approval from the Health Research Ethical Clearance Commission, Faculty of Dental Medicine, University of Airlangga, Surabaya, Indonesia (registration no. 0952/HRECC.FODM/IX/2025).

Study location and time

The preparation and standardization of the FCC were conducted at the Pharmacology Laboratory, Faculty of Veterinary Medicine, University of Gadjah Mada, Yogyakarta, Indonesia. Meanwhile, the *in vivo* experiments, including hydronephrosis modeling, sample collection, renal function assays, urinalysis, and immunohistochemical examinations, were carried out at the Laboratory of Pharmacology, Faculty of Veterinary Medicine, University of Wijaya Kusuma Surabaya, Surabaya, Indonesia (FVM, UWKS). The study was conducted from July to September 2025.

Preparation of fermented *Crescentia cujete*

Crescentia cujete fruit specimens were sourced from the University of Wijaya Kusuma Surabaya area, Surabaya, Indonesia. The fruit pulp was extracted and processed into a fermentation product following the specific protocol described in a previous study (Wilujeng et al., 2023). The fermentation procedure was carried out by mixing fruit pulp with water, pectinase (Pectinex Ultra, UK), and sugar. The components were combined at a ratio of 1,000 mL of water, 400 grams of fruit pulp, 40 grams of sugar, and 40 mL of pectinase. The fermentation process was conducted for 30 days at 25°C. The total choline concentration from the FCC was 114.97 ± 5.14 mg/mL.

Animal models and acclimatization

The present study utilized 30 male Sprague Dawley rats (6 months, 253.76 ± 8.32 grams) obtained from the Laboratory of Pharmacology, FVM, UWKS, Surabaya, Indonesia. The animals were housed in individual cages (30 × 30 × 20 cm) with wood shaving bedding. Prior to the study, the rats underwent a 7-day acclimatization period with *ad libitum* access to standard feed (RatBio®, Indonesia) and drinking water (Cleo®, Indonesia).

Sham-operated procedure

Anesthetic induction was performed using an intraperitoneal ketamine–xylazine regimen (50 and 4 mg/kg BW, respectively; KetA100 and Xyla, Agrovet Market, Peru), following a previously established protocol (Struck et al., 2011). In the sham-operated group, a laparotomy was performed with the rats positioned dorsally. The ventral abdominal area was shaved and disinfected before a midline incision was made. The gastrointestinal tract was briefly retracted and subsequently repositioned after irrigation with physiological saline. To prevent infection, a prophylactic antibiotic combination of penicillin (23 mg/kg BW PenStrep®, Intervet, USA) and streptomycin (38 mg/kg BW, Propen, GlobeVet, UK) was administered intraperitoneally. The administered dose was in accordance with the manufacturer's recommendations. The abdominal wall was closed using simple interrupted sutures with chromic catgut 4.0 (Onemed, Indonesia) for the muscle layer and silk 4.0 (Onemed, Indonesia) for the skin. The incision site was treated with 5% povidone-iodine (Onemed, Indonesia).

Induction of unilateral ureteral obstruction

The hydronephrosis model was established by performing a midline laparotomy followed by ligation of the right ureter, while sham-operated animals underwent an identical surgical procedure except for ureteral ligation. Following retraction of the digestive tract, the right ureter was identified and ligated at the middle section using monofilament thread (Covidien, USA); the left ureter was left intact without ligation. Ligation was performed at two points and anchored to the abdominal muscle. Upon completion, the digestive organs were repositioned, flushed with physiological saline, and the rats received the standard intraperitoneal antibiotic (23 mg/kg BW penicillin and 38 mg/kg BW streptomycin) regimen, and abdominal closure followed the same technique used in the sham-operated group. The rats were then maintained for 14 days until the kidney formed hydronephrosis (Arifianto et al., 2020).

Post-operative care

Following the induction procedures (both sham and UUO), the surgical wounds were treated with a topical application of Bactroban® cream (GSK, Indonesia) for seven consecutive days. Sutures were removed on day 5 post-surgery.

Study design

The rats were randomly allocated into five experimental groups with one group containing six male rats, a healthy control (negative control, T1), a sham-operated group (T2), an untreated UUO group (T3), UUO plus 92.5 mg/kg BW Prive Uricran® (T4, Sengupta et al., 2011), the dosage was converted from the human therapeutic dose to the rat equivalent, and UUO + 5.92 mg/kg BW FCC (T5, Prakoso et al., 2024). The treatment was initiated on day 15 post-induction. The treatment was administered twice daily by oral gavage using a stainless-steel feeding needle for 14 consecutive days until day 29 post-induction.

Sample collection

Serum, urine, and kidney samples were collected on day 30 post-induction. Blood samples were drawn via the retro-orbital sinus (*vena ophthalmica*) under single-dose ketamine anesthesia (50 mg/kg BW, Struck et al., 2011). Blood was collected into Ethylenediaminetetraacetic acid tubes (EDTA tubes, Onemed, Indonesia) for plasma and plain tubes for serum separation. Urine was collected directly from the bladder via cystocentesis using a 3 mL syringe with a 26 G needle (Onemed, Indonesia; Reineke et al., 2021) and stored in Eppendorf tubes. Euthanasia was conducted by administering a lethal intraperitoneal dose of ketamine (150 mg/kg BW KetA-100, Agrovet, Peru). The left kidney was subsequently collected and fixed in 10% neutral buffered formalin (NBF, Leica Biosystems, USA) for histopathological examination.

Renal function and urinalysis assays

Assessment of renal function included the measurement of blood urea nitrogen (BUN) and serum creatinine levels using photometry (Microlab 300, Vital Scientific, Netherlands), with results reported quantitatively (Wijayanti et al., 2024). Urinalysis profiles were examined using a urine analyzer (Urite-50, China) according to the manufacturer's instructions. Evaluated parameters included pH, protein, glucose, ketones, urobilinogen, bilirubin, erythrocytes, nitrites, leukocytes, and specific gravity (SG), reported as semi-quantitative data (Table 1).

Table 1. Standard scoring system for reporting urinalysis

Parameter \ Score	0	1	2	3
Colour	Pale yellow	Dark yellow	Amber	Brown
Leukocytes (Cells/µL)	0 – 10	11 – 25	26 – 500	>500
Ketone (mmol/L)	0.25 – 0.5	>0.5	ND	ND
Nitrite (mg/dL)	<0.06	>0.06	ND	ND
Urobilinogen (µmol/L)	0 – 1	>1 – 33	>33 – 100	>100
Bilirubin (µmol/L)	3.4 – 6.8	>6.8	ND	ND
Protein (g/L)	0.0 – 0.1	>0.1 – 1.00	>1.00 – 2.00	>2.00
Glucose (mmol/L)	0	>0	ND	ND
SG	Reported directly as the output values from the instrument			
Erythrocytes (cells/µL)	0-10	>10-100	>100-200	>200
pH	Reported directly as the output values from the instrument			
Vitamin C (mmol/L)	0.28 – 1.12	>1.12	ND	ND

-: No unit, ND: Not determined, SG: Specific gravity

Immunohistochemical staining

Kidney specimens were dehydrated and cleared before being embedded in paraffin. Sections of 4 µm were

generated and placed on slides coated with poly-L-lysine. For the IHC analysis, the steps followed the method described by Prakoso et al. (2020). After deparaffinization and rehydration, antigen retrieval was performed using Bond Epitope Retrieval Solution (RE7119, Leica Biosystems) at 98°C for 20 minutes. Endogenous peroxidase activity was blocked with 4% H_2O_2 (RE7101), followed by non-specific protein blocking with 0.4% casein (RE7102). Sections were then incubated with primary antibodies against *COX-2* (Sc 19999, Santa Cruz, USA, 1:500) or *VEGF* (Sc 7269, Santa Cruz, USA, 1:300), followed by incubation with secondary antibodies and HRP polymer (RE7111 and RE7112, Leica Biosystems). Antigen visualization was achieved using 3,3′-Diaminobenzidine (DAB) chromogen, followed by hematoxylin counterstaining (RE7107).

Morphometry of immunoexpression of *cyclooxygenase-2* and *vascular endothelial growth factor*

The immunoexpression of *COX-2* and *VEGF* was quantified using ImageJ software (NIH, USA). To ensure objectivity, the analysis was performed by a pathologist in a blinded manner. Immunohistochemistry staining was performed in duplicate on each kidney sample for both *COX-2* and *VEGF* parameters. Five fields of view were captured from each slide at 400× magnification for analysis. Digital images were converted to 8-bit format, and Red, Green, Blue (RGB) color ratios were adjusted to specifically detect immunoreactive areas. Measurements were taken using the "measure area tool" function from the ImageJ software, and results were reported as the percentage (%) of immunoreactive area.

Data analysis

Quantitative data (BUN, creatinine, and urine pH) were analyzed using One-way ANOVA followed by Duncan's post-hoc test. Semi-quantitative data (urinalysis parameters) and the percentage of *COX-2* and *VEGF* immunoexpression were analyzed using the non-parametric Kruskal-Wallis test followed by the Mann-Whitney U test. The statistically significant level was defined as $p < 0.05$.

RESULTS

In the current study, groups T1 and T2 exhibited no differences in BUN and creatinine values when compared to each other. This finding suggests that the laparotomy technique utilized had no adverse effect on renal function, specifically in terms of BUN and creatinine. Moreover, renal function assessments revealed that inducing unilateral hydronephrosis without subsequent therapy (T3) precipitated a marked elevation in BUN to 46.11 ± 6.57 mg/dL and serum creatinine to 1.28 ± 0.70 mg/dL. These values differed significantly from the healthy control group (T1), which maintained baseline levels of 10.73 ± 0.83 mg/dL for BUN and 0.33 ± 0.06 mg/dL for creatinine ($p < 0.05$). The T4 cohort's BUN and creatinine levels were 30.64 ± 2.43 mg/dL and 0.74 ± 0.58 mg/dL, respectively, while the T5 group's levels decreased to 26.47 ± 4.43 mg/dL and 0.50 ± 0.20 mg/dL, respectively, in comparison to the control (T1, $p < 0.05$). However, there were no significant differences in BUN and creatinine levels between groups T4 and T5 ($p > 0.05$). Nevertheless, although these markers were decreased, the renal parameters in the treated groups remained significantly different from the baseline levels observed in the control and sham-operated animals ($p < 0.05$, Table 2).

Regarding urinalysis parameters, the untreated group (T3) exhibited significant deterioration, characterized by elevated scores for leukocytes (2.75 ± 0.50), glucose (1.00 ± 0.0), and nitrites (1.00 ± 0.0) levels far exceeding those of the healthy control group (T1), where all scores remained at 0.0 ± 0.0 ($p < 0.05$). Notably, the treatment administered to the T5 group effectively restored these parameters to near-control conditions. Leukocyte scores returned to 0.0 ± 0.0, glucose dropped to 0.25 ± 0.50, and nitrites decreased to 0.50 ± 0.57, showing no statistical difference from the healthy baseline ($p > 0.05$). Furthermore, while urine SG spiked to 1.0563 ± 0.0 in the T3 group, it normalized to 1.0162 ± 0.01 in the T5 cohort, a value comparable to the sham-operated group (T2, $p < 0.05$, Table 3).

Immunohistochemical analysis of *COX-2* highlighted a statistically significant surge in immunoexpression within the T3 group relative to controls ($p < 0.05$). Qualitatively, it was evidenced by intense reactivity in the epithelium of the proximal convoluted tubules (Figure 1A), marked by maximal dark brown chromogen absorption in the untreated subjects (Figure 1B). Conversely, therapeutic administration in groups T4 and T5 significantly suppressed *COX-2* immunoexpression compared to the control group (T1, $p < 0.05$). Consequently, the qualitative reactivity in the treated groups (T4 and T5) diminished to the point where it was indistinguishable from the patterns observed in the T1 and T2 cohorts ($p < 0.05$, Table 4, Figure 1C-1D).

A parallel trend was observed in the immunoexpression of *VEGF*. The qualitative assessment of immunoexpression of *VEGF* found that the marker was colocalized within the mesangial cells and the tubular epithelium (Figure 2). Moreover, the untreated group (T3) displayed a high density of *VEGF* in kidney tissue (Figure 2B). However, the therapeutic regimens significantly downregulated *VEGF* immunoexpression; both T4 and T5 groups exhibited a gradual

reduction in density, ultimately reaching levels that were not significantly different ($p > 0.05$) from the weak density observed in the healthy control (T1) and sham-operated (T2) groups (Table 4; Figure 2C-2D).

Table 2. The blood urea nitrogen and creatinine levels of rats after 14 days of treatment using fermented *Crescentia cujete*

Parameter (mg/dL)	T1	T2	T3	T4	T5
BUN	10.73 ± 0.83^{a}	11.06 ± 0.60^{a}	46.11 ± 6.57^{c}	30.64 ± 2.43^{b}	26.47 ± 4.43^{b}
Creatinine	0.33 ± 0.06^{a}	0.32 ± 0.09^{a}	1.28 ± 0.70^{c}	0.74 ± 0.58^{c}	0.50 ± 0.20^{b}

T1: Control, T2: Sham-operated, T3: UUO without treatment, T4: UUO plus 92.5 mg/kg BW Prive Uricran®, T5: UUO plus 5.92 mg/kg BW FCC, BUN: Blood urea nitrogen, ^{a,b,c} different superscript letters indicate significant differences in a row ($p < 0.05$).

Table 3. The biochemical parameters of rats after 14 days of treatment using fermented *Crescentia cujete*

Parameter	T1	T2	T3	T4	T5
Colour	0.50 ± 0.57^{a}	0.75 ± 0.50^{a}	2.50 ± 0.57^{c}	1.50 ± 0.57^{b}	1.50 ± 0.57^{b}
Leukocytes	0.0 ± 0.0^{a}	0.0 ± 0.0^{a}	2.75 ± 0.50^{b}	0.25 ± 0.50^{a}	0.0 ± 0.0^{a}
Ketone	0.0 ± 0.0^{a}	0.0 ± 0.0^{a}	0.50 ± 0.57^{a}	0.0 ± 0.0^{a}	0.0 ± 0.0^{a}
Nitrite	0.0 ± 0.0^{a}	0.0 ± 0.0^{a}	1.00 ± 0.0^{b}	0.75 ± 0.50^{b}	0.50 ± 0.57^{a}
Urobilinogen	0.0 ± 0.0^{a}	0.0 ± 0.0^{a}	2.25 ± 0.50^{c}	1.75 ± 0.95^{b}	1.25 ± 0.50^{b}
Bilirubin	0.0 ± 0.0^{a}	0.0 ± 0.0^{a}	0.50 ± 0.57^{a}	0.0 ± 0.0^{a}	0.0 ± 0.0^{a}
Protein	0.0 ± 0.0^{a}	0.0 ± 0.0^{a}	2.75 ± 0.50^{c}	1.00 ± 0.81^{b}	0.75 ± 0.95^{b}
Glucose	0.0 ± 0.0^{a}	0.0 ± 0.0^{a}	1.00 ± 0.0^{b}	0.25 ± 0.50^{a}	0.25 ± 0.50^{a}
SG	1.0150 ± 0.01^{a}	1.0162 ± 0.01^{a}	1.0563 ± 0.0^{b}	1.0188 ± 0.01^{a}	1.0162 ± 0.01^{a}
Erythrocytes	0.0 ± 0.0^{a}	0.0 ± 0.0^{a}	2.75 ± 0.50^{c}	1.00 ± 0.81^{b}	1.00 ± 0.81^{b}
pH	7.53 ± 0.54^{a}	7.37 ± 0.62^{a}	8.77 ± 0.63^{b}	7.69 ± 0.57^{a}	7.73 ± 0.49^{a}
Vitamin C	0.0 ± 0.0^{a}	0.0 ± 0.0^{a}	0.0 ± 0.0^{a}	0.0 ± 0.0^{a}	0.0 ± 0.0^{a}

T1: Control, T2: Sham-operated, T3: UUO without treatment, T4: UUO plus 92.5 mg/kg BW Prive Uricran®, T5: UUO plus 5.92 mg/kg BW FCC, BUN: Blood urea nitrogen, SG: Specific gravity, ^{a,b,c} Different superscript letters indicate significant differences in a row ($p < 0.05$).

Table 4. The immuneexpression of *cyclooxygenase-2* and *vascular endothelial growth factor* of rats after 14 days of treatment using fermented *Crescentia cujete*

Parameter (%)	T1	T2	T3	T4	T5
COX-2	17.09 ± 4.43^{a}	17.63 ± 2.92^{a}	25.31 ± 1.57^{c}	18.54 ± 1.65^{b}	18.20 ± 2.54^{b}
VEGF	32.38 ± 3.12^{a}	31.04 ± 6.07^{a}	59.68 ± 8.73^{b}	38.16 ± 3.60^{a}	39.76 ± 3.00^{a}

T1: Control, T2: Sham-operated, T3: UUO without treatment, T4: UUO plus 92.5 mg/kg BW Prive Uricran®, T5: UUO plus 5.92 mg/kg BW FCC, BUN: Blood urea nitrogen, ^{a,b,c} Different superscript letters indicate significant differences in a row ($p < 0.05$).

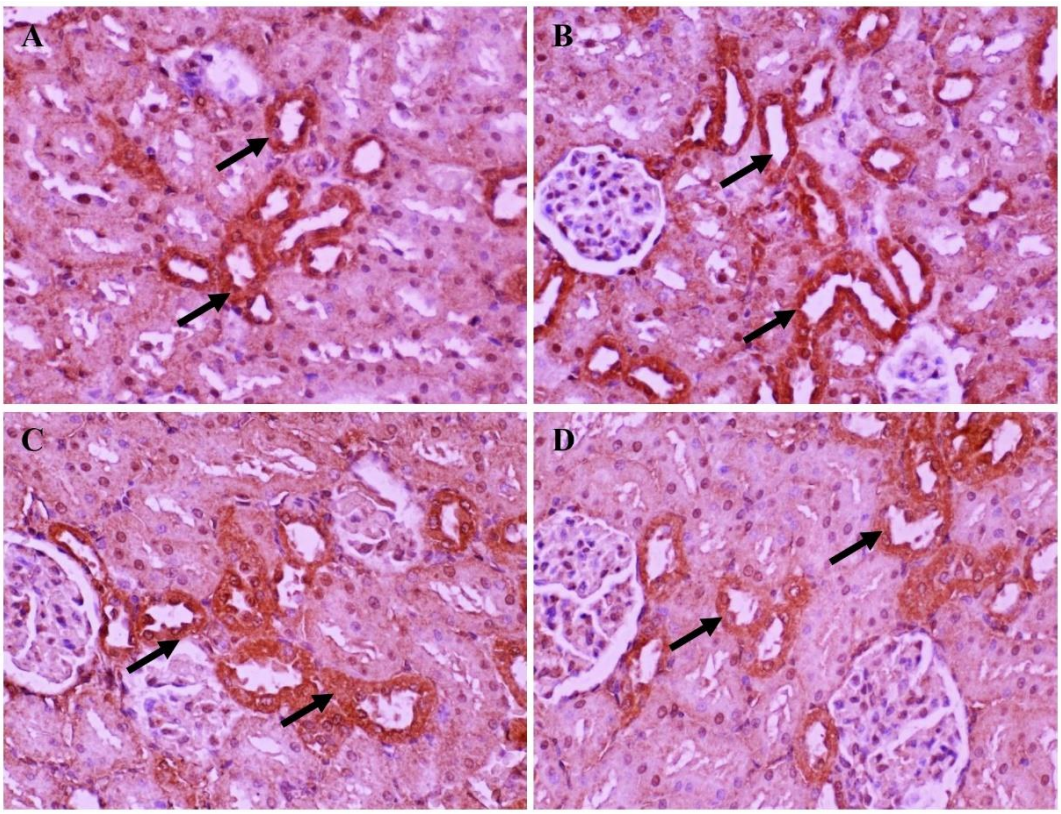

Figure 1. *Cyclooxygenase-2* immunoexpression in the kidneys of rats in a unilateral ureteral obstruction model after 14 days of treatment. **A:** *COX-2* immunoexpression (black arrow) in the control group (T1), **B:** *COX-2* immunoexpression (black arrow) from the untreated group (T3), **C:** *COX-2* immunoexpression (black arrow) from group T4 treated with Prive Uricran® at 92.5 mg/kg BW, and **D:** *COX-2* immunoexpression (black arrow) from group T5 treated with FCC at 5.92 mg/kg BW. Anti-*COX-2* antibody IHC, DAB staining, × 400 magnification (A-D).

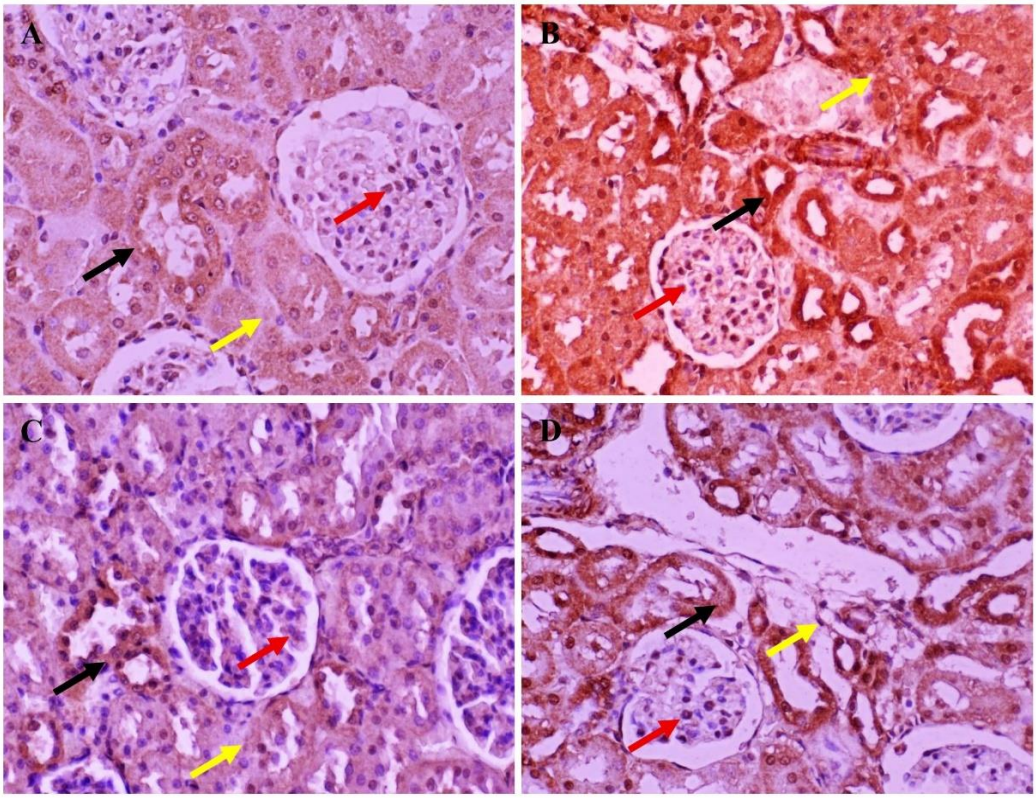

Figure 2. *Vascular endothelial growth factor* immunoexpression in the kidneys of rats in a unilateral ureteral obstruction model after 14 days of treatment. **A:** *VEGF* immunoexpression in the tubular epithelium (black arrow), mesangial cells (red arrow), and interstitium (yellow arrow) of the sham-operated group (T2), **B:** *VEGF* immunoexpression in the tubular epithelium (black arrow), mesangial cells (red arrow), and interstitium (yellow arrow) of the untreated group (T3), **C:** *VEGF* immunoexpression in the tubular epithelium (black arrow), mesangial cells (red arrow), and interstitium (yellow arrow) of the group T4 treated with Prive Uricran® at 92.5 mg/kg BW, and **D:** *VEGF* immunoexpression in the tubular epithelium (black arrow), mesangial cells (red arrow), and interstitium (yellow arrow) of the group T5 treated with FCC at 5.92 mg/kg BW. Anti-*VEGF* antibody IHC, DAB staining, ×400 magnification (A-D).

DISCUSSION

In the current study, unilateral ureteral obstruction in the untreated group (T3) precipitated a cascade of severe renal hemodynamic impairments. The deterioration was clearly manifested as post-renal azotemia, marked by an elevation of serum BUN and creatinine levels (Uchino et al., 2012). Such biochemical derangements point to a critical decline in the Single-Nephron Glomerular Filtration Rate, driven by nephron atrophy in the left kidney under the strain of tubular back-pressure from the obstructed right side (Chevalier et al., 2009). The pathology was further aggravated by urinary stasis in the proximal tubules, which facilitated the passive reabsorption of urea into systemic circulation (Nørregaard et al., 2023). The elevated creatinine levels observed in the UUO model reflect a complete failure of renal clearance compensation in the obstructed kidney, in contrast to the preserved nephron integrity observed in the control (T1) and sham-operated (T2) groups (Arifianto et al., 2020).

To counteract the detrimental compensatory mechanisms and preserve the contralateral kidney, alternative therapeutic interventions using FCC were evaluated in this study. The results were compelling that FCC therapy (T5) demonstrated superior reno-protective efficacy compared to cranberry extract (T4), particularly in stabilizing serum creatinine. While both treatments successfully lowered BUN levels, cranberry extract fell short in mitigating creatinine elevation, suggesting a limited capacity to restore post-obstruction glomerular filtration (Sengupta et al., 2011). In contrast, the pronounced reduction in creatinine observed in the T5 group suggests that FCC exerts a targeted protective effect on the glomerulus. The study hypothesizes that bioactive constituents within FCC, such as alpha-tocopherol and choline, shield podocytes from mechanical stress. The results of the current study align with previous findings indicating that the utilization of alpha-tocopherol protects the nephron from toxicity (Paul et al., 2012). Moreover, Truong et al. (2025) described that acetylcholine, converted from choline, protects podocytes against inflammation and *endothelial* damage. Consequently, FCC, which is rich in choline, maintains a more stable GFR compared to cranberry extract, although full restoration to baseline control levels was not achieved.

The therapeutic interventions led to measurable improvements in urinalysis parameters, as demonstrated by reduced proteinuria and glucosuria, indicating a protective effect on renal function. The untreated T3 group demonstrated increased urinary protein and glucose excretion, indicative of glomerular barrier dysfunction and ischemic alterations in proximal tubular sodium–glucose cotransporter activity (Cunanan et al., 2025). The mechanical stress from increased intraluminal pressure evidently disrupted nephron architecture (Hall and de Seigneux, 2022). However, intervention with FCC effectively reversed these trends, bringing proteinuria and glucosuria scores closer to normal ranges. The recovery signals not only partial glomerular repair and epithelial regeneration in the contralateral kidney but also underscores the potent protective mechanism inherent in the therapy (Moraes Carlesso et al., 2025).

Beyond structural preservation, the study highlighted the role of the urinary environment. The stasis induced by UUO created an environment conducive to secondary infections (Hsu et al., 2022), as evidenced by the alkaline urine (pH 8.77) and positive nitrites found in the untreated UUO group (T3). The findings of the current study demonstrate a significant correlation with the proliferation of urease-splitting bacteria such as *Proteus mirabilis*, which elevate pH and heighten the risk of struvite stone formation (Herout et al., 2023). Fermented *Crescentia cujete* therapy (T5) successfully normalized urinary pH and eliminated nitrite traces, effectively matching the control group's profile. The findings suggest that FCC demonstrates antimicrobial activity against pathogenic organisms and facilitates the recovery of tubular acidification, supporting the maintenance of urinary tract defense mechanisms via antioxidant-mediated pathways (Wijayanti et al., 2024).

The interplay between infection and obstruction also ignited a fierce inflammatory response, characterized by leukocyturia and a surge in *COX-2* immunoexpression within the proximal tubules of the untreated UUO group (T3). While *COX-2*-derived prostaglandins initially help maintain blood flow (Kirkby et al., 2018), the chronic overexpression drives sustained inflammation, macrophage recruitment, and fibrosis on both renal sides (Yang and Li, 2016). In a notable turnaround, FCC therapy suppressed the inflammatory cascade in the contralateral kidney, reducing *COX-2* immunoexpression to levels indistinguishable from healthy controls. The anti-inflammatory action is likely mediated by flavonoids such as quercetin and pinocembrin in *Crescentia cujete*, which inhibit the NF-kB pathway (Gonzales et al., 2023). It is well established that NF-kB is the most essential inducer for *COX-2* synthesis (García-García et al., 2021). Thereby, halting the synthesis of pro-inflammatory prostaglandins and preventing further epithelial damage (Mahendra et al., 2025). Previous studies demonstrate the anti-inflammatory efficacy of FCC by showing significant reductions in inflammatory markers, including *COX-2* and procalcitonin, in pneumonia (Prakoso et al., 2024). Moreover, FCC has been proved as anti-inflammatory potential in reducing circulating *COX-2* and CRP in ischemic stroke (Prakoso et al., 2025).

Finally, the study addressed the hypoxic consequences of obstruction. The vascular compression caused by tubular distension in the UUO model triggered a sharp rise in *VEGF* immunoexpression. The increase of *VEGF* is a

compensatory attempt driven by *Hypoxia-Inducible Factor-1a* (*HIF-1 alpha*, Liu et al., 2022). However, in the fibrotic context of hydronephrosis, the angiogenesis is often maladaptive (Nakagawa et al., 2013), increasing vascular permeability and worsening edema (Miao et al., 2022). Both FCC and cranberry treatments successfully downregulated *VEGF* to baseline levels in groups T1 and T2. The reduction does not imply an inhibition of necessary blood vessel growth, but rather indicates a resolution of the underlying tissue hypoxia (Xu et al., 2025). By preserving tubular structure and reducing edema, FCC compounds such as retinol and alpha-tocopherol probably improved tissue perfusion. A previous study by DiKun et al. (2024) highlighted that retinol and its derivatives, including retinoic acid, reduce kidney tissue fibrosis in nephropathic rat models. Moreover, α-tocopherol plays a crucial role in attenuating hypoxia-driven signaling by mitigating the hypoxic stimulus responsible for excessive *VEGF* upregulation, thereby preventing maladaptive angiogenic responses and further refining the nephroprotective mechanisms in the contralateral kidney following UUO (Rodríguez et al., 2005; Galli et al., 2022).

CONCLUSION

The present findings confirmed the reno-protective potential of FCC in the contralateral kidney following UUO induction, evidenced by the downregulation of BUN and creatinine levels to near-normal values, the successful restoration of urinalysis parameters, and the suppression of *COX-2* and *VEGF* immunoexpression. Future studies should focus on evaluating the therapeutic efficacy of FCC in sub-chronic and chronic models of UUO.

DECLARATIONS

Acknowledgments

The authors acknowledge the research assistants from the Department of Pharmacology, Faculty of Veterinary Medicine, UWKS, Indonesia, for the technical assistance.

Authors' contributions

Oscar Maulana Pribadi and Yos Adi Prakoso designed and supervised the study. Oscar Maulana Pribadi, Yos Adi Prakoso, and Agustina Dwi Wijayanti performed animal model experimentation. Yos Adi Prakoso and Achmadi Susilo performed FCC processing. Yos Adi Prakoso and Sitarina Widyarini conducted unilateral ureteral obstruction in animal models. Oscar Maulana Pribadi and Yos Adi Prakoso collected the sample and analyzed the data. Oscar Maulana Pribadi, Yos Adi Prakoso, and Agustina Dwi Wijayanti performed data interpretation. Yos Adi Prakoso and Sitarina Widyarini performed immunohistochemistry analysis. All authors have read and approved the final version of the manuscript before publication in the present journal.

Funding

The study was partially funded by the Ministry of Education, Culture, Research, and Technology (Kemendikbudristek), Republic of Indonesia (Decree Number: 0070/C3/AL.04/2025; National Grant Number: 128/C3/DT.05.00/PL/2025; Derivative Grant Numbers: 007/LL7/DT.05.00/PL/2025 and 193/PL/LPPM/UWKS/V/2025) and the Post-Doctoral Program 2025 (Funding Number: 4454/UN1.P2/Dit-Lit/PT.01.03/2025).

Competing interests

The authors have not declared any conflict of interest.

Ethical considerations

The data presented in this study are original, and they have not been published elsewhere. The authors did not use AI tools during writing, editing, and preparation of the manuscript.

Availability of the data and materials

Data supporting the findings of the present study are available from the corresponding author upon reasonable request.

REFERENCES

Advani A, Kelly DJ, Advani SL, Cox AJ, Thai K, Zhang Y, White KE, Gow RM, Marshall SM, Steer BM et al. (2007). Role of *VEGF* in maintaining renal structure and function under normotensive and hypertensive conditions. Proceedings of the National Academy of Sciences of the United States of America, 104(36): 14448-14453. DOI: https://www.doi.org/10.1073/pnas.0703577104

Arifianto D, Adji D, Sutrisno B, and Rickyawan N (2020). Renal histopathology, blood urea nitrogen and creatinine levels of rats with unilateral ureteral obstruction. Indonesian Journal of Veterinary Sciences, 1(1): 1-9. DOI: https://www.doi.org/10.22146/ijvs.v1i1.46515

Baltusnikiene A, Staneviciene I, and Jansen E (2023). Beneficial and adverse effects of vitamin E on the kidney. Frontiers in Physiology, 14: 1145216. DOI: https://www.doi.org/10.3389/fphys.2023.1145216

Baris E, Simsek O, Arici MA, and Tosun M (2023). Choline and citicoline ameliorate oxidative stress in acute kidney injury in rats. Bratislavske Lekarske Listy, 124(1): 47-52. DOI: https://www.doi.org/10.4149/BLL_2023_007

Chade AR (2017). Small vessels, big role: Renal microcirculation and progression of renal injury. Hypertension, 69(4): 551-563. DOI: https://www.doi.org/10.1161/HYPERTENSIONAHA.116.08319

Chevalier, R. L., Forbes, M. S., & Thornhill, B. A. (2009). Ureteral obstruction as a model of renal interstitial fibrosis and obstructive nephropathy. *Kidney international*, *75*(11), 1145–1152. DOI: https://www.doi.org/10.1038/ki.2009.86

Cunanan J, Zhang D, Peired AJ, and Barua M (2025). Podocytes in health and glomerular disease. Frontiers in Cell and Developmental Biology, 13: 1564847. DOI: https://www.doi.org/10.3389/fcell.2025.1564847

DiKun KM and Gudas LJ (2023). Vitamin A and retinoid signaling in the kidneys. Pharmacology & Therapeutics, 248: 108481. DOI: https://www.doi.org/10.1016/j.pharmthera.2023.108481

DiKun KM, Tang XH, Fu L, Choi ME, Lu C, and Gudas LJ (2024). Retinoic acid receptor α activity in proximal tubules prevents kidney injury and fibrosis. Proceedings of the National Academy of Sciences of the United States of America, 121(7): e2311803121. DOI: https://www.doi.org/10.1073/pnas.2311803121

Doi K, Noiri E, and Fujita T (2010). Role of *vascular endothelial growth factor* in kidney disease. Current Vascular Pharmacology, 8(1): 122-128. DOI: https://www.doi.org/10.2174/157016110790226606

Galli F, Bonomini M, Bartolini D, Zatini L, Reboldi G, Marcantonini G, Gentile G, Sirolli V, and Di Pietro N (2022). Vitamin E (Alpha-Tocopherol) metabolism and nutrition in chronic kidney disease. Antioxidants, 11(5): 989. DOI: https://www.doi.org/10.3390/antiox11050989

García-García VA, Alameda JP, Page A, and Casanova ML (2021). Role of NF-κB in ageing and age-related diseases: Lessons from genetically modified mouse models. Cells, 10(8): 1906. DOI: https://www.doi.org/10.3390/cells10081906

Gonzales AL, Huang SK, Sevilla UTA, Hsieh CY, and Tsai PW (2023). *In silico* analysis of anti-inflammatory and antioxidant properties of bioactive compounds from *Crescentia cujete* L. Molecules, 28(8): 3547. DOI: https://www.doi.org/10.3390/molecules28083547

Haberal HB and Tonyali S (2024). Factors predicting the need for surgical intervention for hydronephrosis during pregnancy: A systematic review of the literature. Archives of Gynecology and Obstetrics, 309(5): 1801-1806. DOI: https://www.doi.org/10.1007/s00404-024-07391-8

Hall AM and de Seigneux S (2022). Metabolic mechanisms of acute proximal tubular injury. Pflugers Archiv, 474(8): 813-827. DOI: https://www.doi.org/10.1007/s00424-022-02701-y

Herout R, Khoddami S, Moskalev I, Reicherz A, Chew BH, Armbruster CE, and Lange D (2023). Role of bacterial surface components in the pathogenicity of *Proteus mirabilis* in a murine model of catheter-associated urinary tract infection. Pathogens, 12(4): 509. DOI: https://www.doi.org/10.3390/pathogens12040509

Hsu SL, Fan CK, and Liu HY (2022). Obstructive hydronephrosis with secondary urosepsis. Clinical Case Reports, 10(4): e05689. DOI: https://www.doi.org/10.1002/ccr3.5689

Kirkby NS, Sampaio W, Etelvino G, Alves DT, Anders KL, Temponi R, Shala F, Nair AS, Ahmetaj-Shala B, Jiao J et al. (2018). *Cyclooxygenase-2* selectively controls renal blood flow through a novel PPARβ/δ-dependent vasodilator pathway. Hypertension, 71(2): 297-305. DOI: https://www.doi.org/10.1161/HYPERTENSIONAHA.117.09906

Kumar K, Ahmad A, Kumar S, Choudhry V, Tiwari RK, Singh M, and Muzaffar MA (2015). Evaluation of renal histopathological changes, as a predictor of recoverability of renal function following pyeloplasty for ureteropelvic junction obstruction. Nephro-urology Monthly, 7(4): e28051. DOI: https://www.doi.org/10.5812/numonthly.28051

Liu H, Li Y, and Xiong J (2022). The role of hypoxia-inducible factor-1 Alpha in renal disease. Molecules, 27(21): 7318. DOI: https://www.doi.org/10.3390/molecules27217318

Mahendra PGW, Widyarini S, and Prakoso YA (2025). Effects of fermented *Crescentia cujete* and enrofloxacin on inflammation in pneumonic pasteurellosis rats. World Veterinary Journal, 15(4): 978-988. DOI: https://www.doi.org/10.54203/scil.2025.wvj99

Miao C, Zhu X, Wei X, Long M, Jiang L, Li C, Jin D, and Du Y (2022). Pro- and anti-fibrotic effects of *vascular endothelial growth factor* in chronic kidney diseases. Renal Failure, 44(1): 881-892. DOI: https://www.doi.org/10.1080/0886022X.2022.2079528

Mohammadi-Sichani M, Radmanesh F, Taheri S, Ghadimi K, Khodadadi S, Salehi H, Hatampour M, and Kazemi R (2022). Evaluation of glomerular filtration rate decline in patients with renal colic. American Journal of Clinical and Experimental Urology, 10(1): 31-36. Available at: https://pmc.ncbi.nlm.nih.gov/articles/PMC8918396/

Moraes Carlesso R, Cappellari YLR, Boeff DD, da Costa Pereira A, Schmitt Rusch E, de Souza Claudino T, Ritter MR, and Konrath EL (2025). Nephroprotective plant species used in brazilian traditional medicine for renal diseases: Ethnomedical, pharmacological, and chemical insights. Plants, 14(5): 648. DOI: https://www.doi.org/10.3390/plants14050648

Nakagawa T, Sato W, Kosugi T, and Johnson RJ (2013). Uncoupling of *VEGF* with *endothelial* NO as a potential mechanism for abnormal angiogenesis in the diabetic nephropathy. Journal of Diabetes Research, 2013: 184539. DOI: https://www.doi.org/10.1155/2013/184539

Nakamura Y, Kobayashi H, Kanai K, and Abe M (2024). Sudden-onset hypertension leading to the diagnosis of unilateral hydronephrosis due to ureteropelvic junction obstruction. CEN Case Reports, 13(4): 243-248. DOI: https://www.doi.org/10.1007/s13730-023-00832-4

Nørregaard R, Mutsaers HAM, Frøkiær J, and Kwon TH (2023). Obstructive nephropathy and molecular pathophysiology of renal interstitial fibrosis. Physiological Reviews, 103(4): 2827-2872. DOI: https://www.doi.org/10.1152/physrev.00027.2022

Oladunjoye AO, Gberihwa M, and Oyeyinka SA (2025). Fermentation-induced changes in nutritional, antinutritional, and microbial characteristics of calabash fruit (*Crescentia cujete* L.) Seeds. Fermentation, 12(1): 21. DOI: https://www.doi.org/10.3390/fermentation12010021

Paul MV, Abhilash M, Varghese MV, Alex M, and Nair RH (2012). Protective effects of α-tocopherol against oxidative stress related to nephrotoxicity by monosodium glutamate in rats. Toxicology Mechanisms and Methods, 22(8): 625-630. DOI: https://www.doi.org/10.3109/15376516.2012.714008

Prakoso YA, Rini CS, Rahayu A, Sigit M, and Widhowati D (2020). Celery (*Apium graveolens*) as a potential antibacterial agent and its effect on cytokeratin-17 and other healing promoters in skin wounds infected with methicillin-resistant Staphylococcus aureus. Veterinary World, 13(5): 865-871. DOI: https://www.doi.org/10.14202/vetworld.2020.865-871

Prakoso YA, Susilo A, and Widyarini S (2024). The standardization and efficacy of fermented *Crescentia cujete* (L.) in combination with enrofloxacin against artificially induced pneumonic pasteurellosis in rat models. Open Veterinary Journal, 14(12): 3404-3416. DOI: https://www.doi.org/10.5455/OVJ.2024.v14.i12.25

Prakoso YA, Susilo A, Widyarini S, Wahyuningtyas PA, and Hidayah JH (2025). Effects of fermented calabash fruit (*Crescentia cujete* L.) on the Nissl's body, C-RP and *COX-2* in rat models with artificial-induced ischemic stroke. Journal of Research in Pharmacy, 29(5): 2017-2022. DOI:

https://www.doi.org/10.12991/jrespharm.1765113

Rodríguez JA, Nespereira B, Pérez-Ilzarbe M, Eguinoa E, and Páramo JA (2005). Vitamins C and E prevent *endothelial VEGF* and *VEGFR-2* overexpression induced by porcine hypercholesterolemic LDL. Cardiovascular Research, 65(3): 665-673. DOI: https://www.doi.org/10.1016/j.cardiores.2004.08.006

Scott RP and Quaggin SE (2015). Review series: The cell biology of renal filtration. The Journal of Cell Biology, 209(2): 199-210. DOI: https://www.doi.org/10.1083/jcb.201410017

Sengupta KV, Alluri K, Golakoti TV, Gottumukkala G, Raavi J, Kotchrlakota LC, Sigalan S, Dey D, Ghosh S, and Chatterjee A (2011). A randomized, double blind, controlled, dose dependent clinical trial to evaluate the efficacy of a proanthocyanidin standardized whole cranberry (*Vaccinium macrocarpon*) powder on infections of the urinary tract. Current Bioactive Compdounds, 7(1): 39-46. DOI: http://www.doi.org/10.2174/157340711795163820

Siregar S, Mustafa A, and Steven S (2024). Can we predict renal function recovery after pyeloplasty in pediatrics with ureteropelvic junction obstruction? A systematic review. Urology Research and Practice, 50(2): 85-93. Advance online publication. DOI: https://www.doi.org/10.5152/tud.2024.23220

Struck MB, Andrutis KA, Ramirez HE, and Battles AH (2011). Effect of a short-term fast on ketamine–xylazine anesthesia in rats. Journal of the American Association for Laboratory Animal Science, 50(3): 344-348. Available at: https://pubmed.ncbi.nlm.nih.gov/21640029/

Tannuri ACA, Kitahara VKU, Marum AA, Mola B, Souza DFM, Rodrigues LM, Paes VR, Leite KRM, Serafini S, Gonçalves JO et al. (2025). Study of hydronephrosis and renal function reversibility on different development stages of rats that underwent unilateral ureteral obstruction, followed by its release through pyelostomy. Acta Cirurgica Brasileira, 40: e408325. DOI: https://www.doi.org/10.1590/acb408325

Tofteng SS, Nilsson L, Mogensen AK, Nørregaard R, Nüsing R, Diatchikhine M, Lund L, Bistrup C, Jensen BL, and Madsen K (2022). Increased *COX-2* after ureter obstruction attenuates fibrosis and is associated with EP2 receptor upregulation in mouse and human kidney. Acta Physiologica, 235(4): e13828. DOI: https://www.doi.org/10.1111/apha.13828

Truong LD, Trostel J, Roncal C, Cara-Fuentes G, Miyazaki M, Miyazaki-Anzai S, Andres-Hernando A, Sasai F, Lanaspa M, Johnson RJ et al. (2025). Production of acetylcholine by podocytes and its protection from kidney injury in GN. Journal of the American Society of Nephrology, 36(2): 205-218. DOI: https://www.doi.org/10.1681/ASN.0000000000000492

Uchino S, Bellomo R, and Goldsmith D (2012). The meaning of the blood urea nitrogen/creatinine ratio in acute kidney injury. Clinical Kidney Journal, 5(2): 187-191. DOI: https://www.doi.org/10.1093/ckj/sfs013

Wijayanti AD, Prakoso YA, and Isla KJV (2024). Effects of fermented *Crescentia cujete* L. on the profile of hematology, clinical chemistry, and circulatory CD4+/CD8+ in Sprague Dawley rats. Open Veterinary Journal, 14(9): 2475-2483. DOI: https://www.doi.org/10.5455/OVJ.2024.v14.i9.36

Wilujeng S, Wirjaatmadja R, and Prakoso YA (2023). Effects of extraction, fermentation, and storage processes on the levels of choline derived from calabash fruit (*Crescentia cujete* L.). Journal of Research in Pharmacy, 27(2): 620-626. DOI: http://www.doi.org/10.29228/jrp.3443

Xu Y, Xu J, Li J, Kong X, Mao H, Du Z, Zan J, Xu L, Qian W, Ma Z et al. (2025). Interplay of HIF-1α, SMAD2, and *VEGF* signaling in hypoxic renal environments: impact on macrophage polarization and renoprotection. Renal Failure, 47(1): 2561784. DOI: https://www.doi.org/10.1080/0886022X.2025.2561784

Yang T and Li C (2016). Role of *COX-2* in unilateral ureteral obstruction: what is new? American Journal of Physiology Renal Physiology, 310(8): F746-F747. DOI: https://www.doi.org/10.1152/ajprenal.00498.2015

Zeisberg EM, Potenta SE, Sugimoto H, Zeisberg M, and Kalluri R (2008). Fibroblasts in kidney fibrosis emerge via endothelial-to-mesenchymal transition. Journal of the American Society of Nephrology, 19(12): 2282 – 2287. DOI: https://www.doi.org/10.1681/ASN.2008050513

Zhang MZ, Wang S, Wang Y, Zhang Y, Ming Hao C, and Harris RC (2018). Renal medullary interstitial *COX-2* (*cyclooxygenase-2*) is essential in preventing salt-sensitive hypertension and maintaining renal inner medulla/papilla structural integrity. Hypertension, 72(5): 1172-1179. DOI: https://www.doi.org/10.1161/HYPERTENSIONAHA.118.11694